Published in final edited form as:
Dev Biol. 2010 January 15; 337(2): 363–374. doi:10.1016/j.ydbio.2009.11.007.

Role of Epiprofin, a zinc-finger transcription factor, in limb development

Ana Talamillo[1],[6],*, **Irene Delgado**[1],[2],*, **Takashi Nakamura**[3], **Susana de-Vega**[3], **Yasuo Yoshitomi**[3], **Fernando Unda**[4], **Walter Birchmeier**[5], **Yoshihiko Yamada**[3], and **Maria A. Ros**[1],[2]

[1]Departamento de Anatomía y Biología Celular. Facultad de Medicina. Universidad de Cantabria, 39011 Santander, Spain

[2]Instituto de Biomedicina y Biotecnología de Cantabria (IBBTEC). CSIC-UC-IDICAN. Facultad de Medicina. 39011 Santander, Spain

[3]Laboratory of Cell and Developmental Biology, NIDCR, National Institutes of Health, Bethesda, Maryland 20892

[4]Departamento de Biología Celular e Histología, Facultad de Medicina y Odontología, Universidad del País Vasco, 48490 Leioa, Spain

[5]Max-Delbrück Center for Molecular Medicine, Robert-Rössle-Strasse 10, 13092 Berlin, Germany

Abstract

The formation and maintenance of the apical ectodermal ridge (AER) is critical for the outgrowth and patterning of the vertebrate limb. In the present work, we have investigated the role of *Epiprofin* (*Epfn/Sp6*), a member of the SP/KLF transcription factor family that is expressed in the limb ectoderm and the AER, during limb development. *Epfn* mutant mice have a defective autopod that shows mesoaxial syndactyly in the forelimb and synostosis (bony fusion) in the hindlimb and partial bidorsal digital tips. *Epfn* mutants also show a defect in the maturation of the AER that appears flat and broad, with a double ridge phenotype. By genetic analysis, we also show that *Epfn* is controlled by WNT/b-CATENIN signaling in the limb ectoderm. Since the less severe phenotypes of the conditional removal of *b-catenin* in the limb ectoderm strongly resemble the limb phenotype of *Epfn* mutants, we propose that EPFN very likely functions as a modulator of WNT signaling in the limb ectoderm.

Keywords

Epiprofin; Sp6; Sp/KLF; limb development; Apical ectodermal ridge; AER; syndactyly; oligodactyly; WNT/b-CATENIN; BMP

Author for correspondence: M. A. Ros Instituto de Biomedicina y Biotecnología de Cantabria (IBBTEC). CSIC-UC-IDICAN Facultad de Medicina. 39011 Santander. SPAIN Phone: 34 942 201933 Fax: 34 942 201903 rosm@unican.es.
[6]Present address: CIC bioGUNE. Unidad Genómica Funcional. Parque Tecnológico de Bizkaia. Edificio 801A. 48160 Derio, Spain
*These authors contributed equally to this work

INTRODUCTION

The apical ectodermal ridge (AER), a specialized thickened epithelium at the distal edge of the developing limb bud, is a major signaling center for limb development. The AER, through the production of several members of the fibroblast growth factor (FGFs) family, controls appropriate gene expression, survival, and proliferation of the subjacent mesoderm (Niswander, 2003; Tickle, 2003; Saunders, 1948; Dudley et al., 2002, Rowe et al., 1982; Mariani et al., 2008). In the chick, several FGFs have been shown capable of substituting for AER function (Niswander et al., 1993; Fallon et al., 1994; Martin, 1998). In the mouse, the genetic removal of a significant amount of FGF signaling from the AER results in the absence of limbs (Sun et al., 2002; Boulet et al., 2004; Mariani et al., 2008).

The formation of the AER is a complex process that includes the induction of the AER precursor cells. In the mouse, these are initially located in the ventral ectoderm (Kimmel et al., 2000), but are later positioned and compacted at the dorso-ventral tip of the limb bud to form the linear and thickened mature AER (Loomis et al., 1998; Kimmel et al., 2000; Fernández-Teran and Ros, 2008).

The establishment of the AER is directed by complex interactions between the FGF, WNT/b-CATENIN, and BMP signaling pathways, which operate within the ectoderm as well as between the ectoderm and mesoderm components of the early limb bud. Furthermore, this process is linked to the initiation of the limb bud and to the establishment of dorso-ventral (DV) patterning. It is currently accepted that an ectodermal active WNT/b-CATENIN pathway is required for both AER induction and maintenance in the chick and the mouse (Soshnikova et al., 2003; Barrow et al., 2003; Kawakami et al., 2001). BMP signaling is also essential for induction of the AER, probably through action upstream of WNT signaling (Ahn et al., 2001; Soshnikova et al., 2003; Barrow et al., 2003; Pizette et al., 2001). Paradoxically, once the AER has been induced, further BMP signaling becomes detrimental to AER maintenance and is involved in AER regression (Pizette et al., 2001; Zuñiga et al., 1999; Fernández-Teran and Ros, 2008).

Despite this intensive study, the genetic mechanisms that regulate AER formation and maintenance are not yet fully understood. In particular, very few transcription factors have been indentified for these processes. In this context, the importance of SP8, one member of the SP family of transcription factors, has been indicated for AER maintenance and maturation (Bell et al., 2003; Treichel et al., 2003; Kawakami et al., 2004). The SP protein subfamily is characterized by a highly conserved carboxy-terminal DNA binding domain composed of three Cys2His2 zinc finger motifs and a buttonhead box located N-terminal to the zinc finger domain. The amino-terminal region is more variable and contains transcriptional activation or repression domains (reviewed in Suske et al., 2005; Kaczynski et al., 2003; Kadonaga et al., 1987; Wimmer et al., 1993). In addition to *Sp8*, other *Sp* family members, including *Sp5*, *Sp9* and *Epiprofin* (*Epfn/Sp6*), are also expressed in the limb bud (Harrison et al., 2000; Nakamura et al., 2004; Bell et al., 2003; Treichel et al., 2001; Kawakami et al., 2004). The present study was aimed at characterizing the function of *Epfn/Sp6* in limb development.

We show that the limbs formed in the absence of *Epfn* exhibit an altered digital pattern that is characterized by mesoaxial syndactyly, including synostosis in the hindlimb and a partial dorsalization of the digital tips. These limbs develop with a defect in the maturation of the AER, which adopts a double ridge phenotype. By genetic analysis, we also show that *Epfn* is downstream of WNT/b-CATENIN while it does not require FGF signaling for expression. All our results fit with the *Epfn* phenotype resulting from a mild deficit of WNT signaling in the limb ectoderm that affects BMP signaling but not FGF signaling.

MATERIALS AND METHODS

Mutant mice

The generation of *Epiprofin* (*Epfn/Sp6*) mutant mice is described in Nakamura et al., 2008. *Brn4Cre;DN-b-catenin*, *Brn4Cre;b-catenin*$^{flox/flox}$ and *Axin2-LacZ* reporter mice, which express *lacZ* under the control of the endogenous *Axin2* promoter (Soshnikova et al., 2003), were also used in this study. All mice were maintained on a mixed genetic background and genotyped based on previously published reports. *Msx2Cre;Fgf4;Fgf8* mutant embryos (Sun et al., 2002) were kindly provided by Gail Martin and Francesca Mariani and *Fgf10* mutant embryos (Sekine et al., 1999) by Thomas Shimmang.

Skeletal Preparations, *in situ* hybridization and measurements of the limb

After removing skin and visceras, mouse embryos were fixed in 95% ethanol. Alizarin Red and Alcian blue skeletal staining was performed according to standard protocols, cleared by KOH treatment and stored in glycerol. In situ hybridization (ISH) was performed in whole-mount and in sections following standard procedures. At least two specimens for each gene and stage were analyzed. The length of the AER was measured on *Fgf8* hybridized *Epfn* mutant and wild type limbs of equivalent stage using the measure tool from Image J software. The wild type value was considered as 100.

Cell death and cell proliferation assays

Detection of cell death was performed in sections of paraffin-embedded tissue using terminal deoxynucleotidyl transferase mediated dUTP nick-end labelling (TUNEL) with the Apoptag Fluorescein Direct In Situ Apoptosis Detection Kit (Intergen) following the manufactured instructions. Analysis of cell death was also performed in whole limb buds using LysoTracker (Molecular Probes L-7528, Invitrogen). The limb buds were incubated with 5 μl/ml LysoTracker solution in HBSS at 37°C for 30 minutes before been fixed in 4% PFA and analyzed.

Detection of cell proliferation in sections was performed by immunohistochemical assay using the anti phosphorylated histone H3 antibody (rabbit polyclonal Phospho H3 from Upstate Biotechnology, USA) diluted at 1/100.

RESULTS

Pattern of expression of *Epiprofin* in the developing limb

Epfn is expressed in proliferating dental epithelium during early tooth development, in the matrix of hair follicles, and in the AER of the limb (Nakamura et al., 2004; 2008; Hertveldt et al., 2008). Since we were interested in studying the function of *Epfn* during limb development, we first analyzed in detail its spatial and temporal pattern of expression, by *in situ* hybridization.

At E9, prior to the emergence of the forelimb bud, *Epfn* was strongly expressed in the prospective limb ectoderm, at both the fore and hind limb levels (Fig. 1A). The expression was similar in the dorsal and ventral ectoderm, as shown in the section at forelimb level in Fig. 1B (the level of the section is indicated in Fig. 1A). After the initial limb budding at E9.5, *Epfn* expression continued throughout the entire limb ectoderm, but with a higher level of expression in the ventral ectoderm (Fig. 1C). This could be clearly observed in transverse sections (Fig. 1D; the level of the section is indicated in Fig. 1C). From E10 on, *Epfn* expression progressively declined, first from the dorsal and then from the ventral ectoderm. By E11.5, its expression was mainly confined to the AER (Fig. 1E–F). At later stages, *Epfn* expression was observed to extend from the AER into the dorsal and ventral

ectoderm, predominantly at the tip of the digits, while its expression gradually faded over the regressing interdigits (E12.5, Fig. 1G). At E15.5, *Epfn* expression continued to persist over the tip of the digits (Fig. 1H). Notably, *Epfn* expression was always restricted to the limb ectoderm, as confirmed through the analysis of sections of hybridized embryos (Fig. 1B, D and not shown).

At intermediate stages of limb development, in particular, the pattern of expression of *Epfn* was very similar to that of *Fgf8* (Fig. 1E–F; Crossley and Martin, 1995), although the domain of expression of *Epfn* was wider than that of *Fgf8* and extended further into the dorsal and ventral ectoderm. In light of this similarity in expression pattern between *Fgf8* and *Epfn* (Fig. 1A–F; Crossley and Martin, 1995), and their very early activation in the presumptive limb ectoderm, we investigated which gene was activated first. To precisely compare relative activation times, we performed *in situ* hybridization to *Epfn* and to *Fgf8* in consecutive transverse tissue sections (6 micrometers apart) at the forelimb level of E9 embryos. *Epfn* expression was activated earlier than *Fgf8* in the limb ectoderm (Fig. 1I–J). Its expression also continued at the tip of the digits, well after *Fgf8* expression had ceased (Fig. 1H; Crossley and Martin, 1995), indicating that neither the activation nor the maintenance of *Epfn* expression in the limb ectoderm required *Fgf8* expression.

Overall, the pattern and dynamics of *Epfn* expression in the limb ectoderm suggests its possible involvement in the establishment and/or maintenance of the AER.

Limb defects in the *Epiprofin*$^{-/-}$ mice

To investigate the biological role of *Epfn* during limb development, we analyzed the limb phenotype of mice that had a targeted deletion of the *Epfn* gene (Nakamura et al., 2008).

At birth, the limbs of homozygous *Epfn* mutants showed a normal external morphology, apart from some abnormalities of the digits (Fig. 2). In the forelimbs, these abnormalities consisted of soft-tissue syndactyly of digits 2 and 3, and occasionally digit 4 (arrowhead in Fig. 2B; control in Fig. 2A). In the hindimbs, these abnormalities were characterized by oligodactyly of four digits due to the fusion of digits 3 and 4 although there were cases in which the fusion was not complete (Fig. 2D; control in Fig. 2C). The penetrance was of 60% and the expressivity variable, with the majority of affected specimens exhibiting the phenotype only on their left side; however, some mutants with a strong phenotype showed both sides equally affected.

The examination of skeletal preparations of homozygous *Epfn* mutant neonates, in comparison with control littermates, demonstrated a normal skeletal pattern in the forelimbs (Fig. 2E–F). The soft tissue syndactyly was not always observed during the skeletal preparations because sometimes the removal of the skin untied the digits (arrowhead in Fig. 2F). In some specimens, secondary osseous fusion of the abnormally closed distal phalanges of forelimb digits 2 and 3 was also observed (not shown). The skeletal preparation of the hindlimbs showed that oligodactyly was caused by the synostosis (osseous fusion) of digits 3 and 4 from the level of the proximal phalanx (Fig. 2G–H). The heads (distal ends) of metatarsals 3 and 4 appeared twisted toward each other and participated in a single metatarso-phalangeal joint with a very thick proximal phalanx, presumably resulting from the fusion of the proximal phalanges of digits 3 and 4 (Fig. 2H). Remarkably, we found a gradation in the fusion of digits 3 and 4 that ranged from the complete fusion (Fig. 2H) to a much milder phenotype in which digits 3 and 4 were closely apposed together, but still individually identifiable (see also Fig. 8E–H).

Epfn mutant limbs also exhibited a DV broadening of the distal tip of central digits (Fig. 2J). This broadening merely consisted of an abnormal distal DV split of the ungueal phalanx,

accompanied by an altered morphology of the claw (Fig. 2I–L). Remarkably, the hyponychium adopted the morphology of the keratinized dorsal nail plate, reflecting a dorsalized morphology (Fig. 2I–L), while conical nails were never observed.

Finally, it should be noted that the limbs of the heterozygous littermates always displayed a normal phenotype, indicating the recessive inheritance of this gene. In homozygotes, the stylopod and the zeugopod were of normal morphology, as phenotypic alterations were always restricted to the mesoaxial region of the autopod; digits 1 and 5 always appeared normal. In summary, the limb phenotype of *Epfn* mutants was characterized by mesoaxial syndactyly, cutaneous in the forelimb and osseous in the hindlimb, and partial bidorsalization of the digital tips. Taken together, our results reveal a role for *Epfn* in the morphogenesis of the autopod.

Defective AER morphogenesis in the absence of *Epiprofin*

Since *Epfn* is expressed in the limb ectoderm, including the AER progenitors and later the mature AER, we next analyzed the possible morphological and molecular consequences of *Epfn* removal on the formation of the AER. The histological analysis at E11.5 of both fore (Fig. 3B) and hind (Fig. 3C) mutant limbs revealed the presence of an abnormal AER that appeared expanded (broader) in the DV axis (marked by arrowheads in Fig. 3B–C) and that lacked the characteristic elevation of the normal mature AER (compare Fig. 3B–C with Fig. 3A). In some locations, the mutant AER even protruded into the mesoderm (arrowheads in Fig. 3D).

Since *Fgf8* is considered a crucial marker for the AER, we analyzed *Fgf8* expression in *Epfn* mutants and control littermates (n= 6, Fig. 3E–L). In agreement with the histological analysis, mutant embryos exhibited a DV expanded domain of *Fgf8* expression in both fore- and hindlimb buds (shown for E11, Fig. 3F, H), compared with wild type (Fig. 3E, G). Generally, *Fgf8* expression was observed in two parallel stripes at the borders of the expanded AER, in a typical “double ridge” appearance (Fig. 3E–F). Sections of the hybridized embryos showed that the central part of the AER, which corresponded to the part that sometimes protruded into the mesoderm, lacked *Fgf8* expression (Fig. 3E–F, inserts).

In addition to the altered AER morphology, we also observed a reduction in the AP length of the mutant AER. This could be evaluated by the length of the *Fgf8* expression domain (an average of 68% in the mutant relative to 100% in the wild type, n=3; Fig. 3I–L), which correlated with a corresponding reduction in the AP axis of the mutant limb. Thus, in the absence of *Epfn*, both the width and the length of the AER were affected and the limbs became reduced in the AP axis but wider in the DV axis.

The expression of *Fgf8* appeared weaker in some *Epfn* mutants (Fig 3F, H), which raised the question of whether this was just a reflection of the flattened AER or whether it was a real reduction in the level of *Fgf8* expression. Thus, we decided to assess the FGF signaling level by evaluating the expression of *Dusp6* (also known as *Mkp3*) and *Sprouty4* (*Spry4*) in the limb bud mesoderm, as they are considered good readouts of FGF signaling (Kawakami et al., 2003; Eblaghie et al., 2003; Mariani et al., 2008). *Dusp6* and *Spry4* expression occurred in mutant fore- and hindlimb buds similar to normal (shown respectively for E10.5 and E11.5 in Supplementary Fig. 1). These results indicated that the production of FGF in the AER was not significantly modified.

Since expansion in the AP axis is controlled by SHH, we also examined *Shh* expression and signaling in *Epfn* mutant limbs. We found that *Shh* expression was initiated in the mutant limb normally and that the domain of expression was within the normal limits in both the fore- and hindlimbs of mutant limbs (Supplementary Fig. 2A–D). Small differences in the

domain of expression between mutants and wild type limb buds always correlated with small differences in developmental age (Supplementary Fig. 2C–D). To assess Shh signaling we analyzed the expression of *Gli1* and *Ptc1*, targets of Shh, which showed a normal pattern in mutant limbs, indicating normal Shh signaling in the mutant mesoderm (Supplementary Fig. 2). This ruled out a substantial participation of SHH in the reduction of the AP extension of the AER, and pointed to a defect in the architecture of the limb secondary to the flattened AER, rather than to a defect in the expansion of the limb bud.

In summary, our results showed that the induction of the AER occurred in *Epfn* mutants, but that the compaction of AER cells failed and, consequently, the morphology of the mature AER was never achieved. Therefore, *Epfn* mutant limbs developed with an abnormally broad and flat AER with reduced AP extension, in association with the corresponding change in the overall shape of the mutant limb bud. Finally, it should be noted that the double ridge phenotype was fully penetrant, as we observed it in all homozygous embryos analyzed.

Epiprofin expression in the limb ectoderm is under the control of WNT/b-CATENIN signaling

In order to further investigate the role of EPFN in AER development, we analyzed the regulation of *Epfn* expression in the limb ectoderm. We first addressed its relationship with b-CATENIN, a central component of the canonical WNT signaling pathway that is known to be involved in AER induction and maintenance (Soshnikova et al., 2003; Barrow et al., 2003; Hill et al., 2006; Kawakami et al., 2001). For this purpose, we analyzed the expression pattern of *Epfn* in mutants with gain-of-function of *b-catenin* in the limb ectoderm (*Brn4Cre;DN-b-catenin*). These mutants have been described (Soshnikova et al., 2003) as showing an expanded AER with strong expression of *Fgf8*. In contrast, mutants with loss-of-function of *b-catenin* in the limb ectoderm (*Brn4Cre*;*b-catenin* $^{flox/flox}$) show a defect in AER formation, with reduced or absent *Fgf8* expression (Soshnikova et al., 2003). *Epfn* expression in the hindlimb of the *b-catenin* gain-of-function mutant was markedly expanded in association with the expansion of the AER (n=2, Fig. 4B), while in the loss-of-function mutant limb, its expression was reciprocally reduced in accordance with the AER alteration and undetectable in the more severe cases (n=2, Fig. 4C). These changes in *Epfn* expression are identical to those reported for *Fgf8* (compare Fig. 4A–C with Fig. 2 in Soshnikova et al., 2003) and indicate that WNT/b-CATENIN signaling in the limb ectoderm is absolutely required for *Epfn* expression, as has been shown for *Fgf8* (Soshnikova et al., 2003; Barrow et al., 2003).

Due to the tight regulation of *Epfn* by WNT/b-CATENIN signaling in the limb ectoderm, we asked whether WNT signaling might be impaired by the absence of EPFN. For this purpose, we decided to analyze the state of canonical WNT signaling in the *Epfn* mutant limb by analyzing the expression of *Dkk1*, *Lef1* and *Axin2*, considered good targets of WNT/b-CATENIN signaling.

We found that *Dkk1* was normally expressed in mutant limbs at E10.5 and E11.5 (n=4, Fig. 4D and not shown). However, by E12, *Dkk1* expression appeared to have been upregulated in a distal rim of subridge mesoderm, particularly in the hindlimb (n=2, arrows in Fig. 4E). This upregulation was clearly appreciated in sections of the hybridized embryos, as shown in the inserts in Fig. 4E. Since *Dkk1* is a negative regulator of WNT/b-CATENIN signaling, this finding fits with a reduction in WNT/b-CATENIN signaling in *Epfn* mutant limb (Niida et al., 2004, González-Sancho et al., 2005). The expression of *Lef1*, a direct target of WNT/b-CATENIN, was similarly expressed in E11.5 mutant and wild type limbs (n=2, Fig. 4F). We also examined the expression of *Axin2*, another direct target of WNT/b-CATENIN (Jho et al. 2002; Lustig et al. 2002), using mice that carry a *LacZ* gene in the *Axin2* locus. *Axin2*

expression was observed in the mutant AER (arrows in Fig. 4G, n=2), although a moderate reduction in expression was appreciable not only in the AER, but also in the dorsal and ventral ectoderm. We note that the reduction in *Axin2* expression in the mutant AER could be due, at least partially, to the flattened AER phenotype. All of these data indicate that the absence of EPFN caused a moderate reduction in the WNT/b-CATENIN signaling level in the limb ectoderm, which fits nicely with by the phenotypic traits.

Epiprofin expression is independent of FGF signaling

WNT/b-CATENIN signaling in the limb ectoderm is required for *Epfn* (Fig. 4A–C) and for *Fgf8* expression (Soshnikova et al., 2003; Barrow et al., 2003). Since we have also shown that *Fgf8* is expressed in the absence of *Epfn* (Fig. 3E–L), we hypothesized that *Epfn* could function downstream FGF signaling in the limb ectoderm, as has been shown for *Sp8*, another member of the SP/KLF family also expressed in the limb ectoderm (Kawakami et al., 2004). To test this hypothesis, we analyzed the expression pattern of *Epfn* when FGF production in the limb ectoderm is significantly reduced, using the *Msx2-cre;Fgf4;Fgf8* double knockout mice (Sun et al., 2002). It has been shown that the expression of *Msx2-cre* is different in fore and hindlimbs. In the hindlimb, *Msx2-cre* is expressed early enough to produce a complete inactivation of *Fgf4* and *Fgf8* before they are expressed, while in the forelimb, *Msx2-cre* functions after expression of *Fgf8* and *Fgf4* have been initiated (Sun et al., 2002). Despite this difference, *Epfn* was expressed in the AER of both the fore and hindlimbs of these double knockout mice, analyzed at E10 (n=2, Fig. 5A–D). Indeed, the expression was stronger than normal in the forelimb, in agreement with the hyperplastic AER typical of these mutants (Fig. 5A–B, Sun et al., 2002).

Since *Sp8* has also been shown to be downstream of FGF10 signaling from the mesoderm, we also analyzed *Epfn* expression in *Fgf10* knockout mice (Sekine et al., 1999). *Fgf10* mutants do not form a limb but the initial budding does occur. We found that *Epfn* was normally expressed in the limb ectoderm in the absence of *Fgf10* (n=2, Fig. 5E–F). Therefore, these results provided genetic evidence that *Epfn* expression in the limb ectoderm is independent of *Fgf4* and *Fgf8*, which conjointly represent the majority of FGF signaling from the AER. *Epfn* initiation of expression is also independent of *Fgf10*, which represents FGF signaling from the subjacent mesoderm.

In summary, the results of these genetic studies indicate that *Epfn* is downstream of WNT/b-CATENIN signaling in the limb ectoderm while it does not require FGF signaling for expression. It should be noted that *Fgf9* and *Fgf17* remain expressed in the double *Fgf4;Fgf8* mutant AER and could, therefore, support *Epfn* expression. In this regard, the analysis of AER-*Fgfr2* conditional KOs would be necessary to completely rule out a FGF requirement for *Epfn* expression.

The possibility that the transcription factor EPFN could mediate WNT/b-CATENIN dependent induction of *Fgf8* in the limb ectoderm was raised, but was not supported due to the fact that *Fgf8* is expressed in the expanded AER of *Epfn* mutants. However, it should be considered that the related factor SP8, which has a similar pattern of expression, could perform redundant functions with EPFN/SP6, if its expression was retained in the absence of *Epfn*. Indeed, *Sp8* has been shown to function downstream of WNT/b-CATENIN (Bell et al., 2003; Treichel et al., 2003) and to regulate *Fgf8* expression in the chick limb bud (Kawakami et al., 2004). Therefore, to investigate the state of *Sp8* expression in the absence of *Epfn,* we analyzed *Sp8* expression in *Epfn* mutants. *Sp8* expression was normal in *Epfn* mutant limbs (Supplementary Fig. 3, n=3), indicating that it is independent of EPFN, and raising the possibility that SP8 could substitute for EPFN in mediating WNT/b-CATENIN functions in the limb ectoderm.

Late dorso-ventral defects in *Epiprofin* mutants

To analyze DV patterning in *Epfn* mutant limbs, we used the transcription factor LMX1B, which is expressed in the dorsal mesoderm (Fig. 6A; Chen and Johnson, 2002). In early developing *Epfn* mutant limb buds, *Lmx1b* expression remained restricted to the dorsal mesoderm, in a manner comparable to wild type embryos, as shown in Fig. 6A–C for E11.5 hindlimb buds (n=5). However, at later stages (E14.5), occasional patches of ectopic *Lmx1b* expression were detected in the distal ventral mesoderm of mutant limbs, but never in wild type limbs (arrows in Fig. 6D–F, n=2). Since *Epfn* is expressed in the ectoderm and *Lmx1b* expression is regulated by *Wnt7a* expression from the ectoderm, we decided to analyze whether ectopic *Wnt7a* preceded the ventral misexpression of *Lmx1b* (Parr and McMahon, 1995). *Wnt7a* expression was normally restricted to the dorsal ectoderm in early mutant limbs (n=3; Fig. 6G–H). During later stages, the distribution of *Wnt7a* transcripts in the dorsal ectoderm became more diffuse and eventually undetectable both in mutant and wild type limbs (Witte et al., 2008), but ectopic ventral expression was never detected in mutants (not shown). Therefore, in the absence of *Epfn*, DV patterning was normally established in the early limb bud, but eventually ectopic patches of ventral *Lmx1b* expression, independent of *Wnt7a* expression, appeared. As these patches were also observed in digit 5 (Fig. 6F), which never showed the partial bidorsal phenotype, it seems reasonable to consider them a different manifestation of the DV alterations in the mutant, rather than the cause of the bidorsal phenotype. With these exceptions, the overall DV morphology of the limb appeared normal, including the ventral flexion of the joints.

Bidorsalization of the distal tip of the digits is characteristic of the loss of BMP signaling in the limb ectoderm (Pajni-Underwood et al., 2007; Wang et al., 2004). BMP signaling has also been shown to be involved in AER induction and maturation, in delimiting the boundaries of the AER, in regulating digit number and identity and in controlling FGF signaling from the AER (Ahn et al., 2001; Pizette et al., 2001; Wang et al., 2004; Selever et al., 2004; Ovchinnikov et al. 2006; Pajni-Underwood et al., 2007). Therefore, we decided to examine Bmp gene expression in *Epfn* mutant mice. We did not detect differences in *Bmp2* and *Bmp7* expression in mutant limbs (not shown). However, *Bmp4* expression in the mutant mesenchyme was slightly downregulated at E10.5 (n=2; Fig. 7 A–B) and clearly diminished at E11.5 (n= 3, Fig. 7C–D), compared with wild type embryos. *Bmp4* expression in the mutant AER reflected the double ridge phenotype (anterior views in Fig. 7C–D) and at later stages appeared patchy and discontinuous (E12.5, arrows in Fig. 7E–F). Accordingly, the expression of *Msx2*, a downstream target of BMP signaling, was appreciably reduced in the *Epfn* mutant limb mesoderm, confirming a reduction in BMP signaling in the mutant limb (Fig. 7G–H) and showing that the absence of EPFN in the ectoderm had also an impact in the mesoderm.

Cell death and cell proliferation in the *Epiprofin* mutant limb

Modifications in cell proliferation and in cell death have been considered to be causes of syndactyly (Zuzarte-Luis and Hurle, 2005; Lu et al., 2006, Talamillo et al., 2005). Therefore, to evaluate the syndactyly phenotype in more depth, we analyzed cell proliferation and cell death in the *Epfn* mutant limb bud, using immunohistochemistry with the anti phospho-histone H3 (apH3) antibody and the TUNEL assay, respectively, in adjacent tissue sections. At E11 and E12 we found no appreciable differences in the distribution and density of mitotic cells in mutant and wild type fore or hindlimbs (shown in Fig. 8A–B for forelimbs and data not shown). The distribution of apoptotic cells was also found to be similar to normal at these stages in *Epfn* mutants (Fig. 8C–D), which showed the normal apoptotic areas similar to normal (Fernandez-Terán et al., 2006).

The expression pattern of *Sox9*, a marker of cells committed to the chondrogenic lineage (Bi et al., 1999; Akiyama et al., 2002), clearly illustrated that the syndactyly of *Epfn* mutants was established at about the time of, or prior to, the specification of the phalanges and interdigital spaces. By E13, *Sox9* expression in mutant hindlimbs showed the abnormal fusion of prospective digits 3 and 4 (Fig. 8E–F) that consistently occurred from the metatarsal heads. At earlier stages, i.e., at E12, *Sox9* expression revealed the abnormal proximity of the digital condensations for digit 3 and 4 (Fig. 8G–H). These results demonstrate that in the hindlimb the phenotype had already been established prior to the initiation of interdigital cell death; therefore, modifications in interdigital cell death cannot be claimed to be causal to the phenotype. In the case of the synostosis, the interdigital space between digits 3 and 4 never formed in the mutant hindlimb (Fig. 8E–F).

In the forelimbs, digits 2 and 3 and occasionally also digit 4, developed closer than normally with a narrower interdigital space that showed retarded or reduced cell death, as can be observed in the wholemount cell death analysis performed with LysoTracker at E13.5 (Fig. 8I–J). Therefore, a reduction in the normal interdigital cell death could potentially play a role in the establishment of the cutaneous syndactyly of mutant forelimbs.

DISCUSSION

This study provides compelling evidence for an ectodermal role of *Epfn/Sp6* in the process of AER maturation since it is normally expressed in the limb ectoderm and in the AER, and its expression is required to achieve the elevated and compacted morphology typical of the mature AER. EPFN is also required for the correct morphogenesis of the digits. By genetic analysis, we demonstrated that *Epfn* is downstream of WNT/β-CATENIN signaling and that it does not require significant FGF signaling for expression. These observations, together with the similarity between the limb phenotype of *Epfn* mutant and specimens with a mild loss-of-function mutation of õ*catenin* in the limb ectoderm, suggest that the transcription factor EPFN likely function by modulating WNT signaling in the limb ectoderm.

Epiprofin as a candidate to mediate the connection between the WNT and BMP signaling pathways in the limb ectoderm

A regulatory pathway connecting WNT/b-CATENIN signaling and *Fgf8* expression operates both in mouse and chick limb ectoderm to establish the AER (Kawakami et al., 2001; Barrow et al., 2003; Soshnikova et al., 2003; Hill et al., 2006). However, it is well known that there is not a simple linear relationship between ectodermal WNT/b-CATENIN signaling and *Fgf8* and that WNT/b-CATENIN has additional functions such as the activation of the BMP signaling pathways in dorso-ventral patterning (Barrow et al., 2003; Soshnikova et al., 2003). By genetic analysis we demonstrate that *Epfn* expression in the limb ectoderm is downstream of WNT/b-CATENIN signaling while it does not require significant FGF signaling. These observations, together with the fact that *Fgf8* is still expressed in the limb ectoderm in the absence of *Epfn,* places EPFN as an excellent candidate to mediate other WNT functions in the limb ectoderm different from inducing *Fgf8*.

Remarkably, the limb phenotype of *Epfn* mutant embryos is very similar to that shown by the less affected individuals in the *Brn4Cre*-induced loss-of-function mutation of õ*catenin*(Soshnikova et al., 2003). These least affected individuals are missing one central digit in the hindlimb and show bidorsal distal tips. This similarity suggests that the *Epfn* phenotype could result from subtle modifications in WNT signaling as indicated by the subtle modifications in *Axin2* and *Dkk1* expression we have detected.

While the modifications in WNT signaling produced in the absence of *Epfn* are very subtle, FGF signaling appears to remain unmodified. This is supported by the expression of *Dusp6* and *Spry4*, presently considered good readout of FGF signaling, in *Epfn* mutant limbs, as well as by the phenotypic traits that are not typical of *Fgf* mutants. It should be noted however that the related factor SP8 remains expressed in the limb ectoderm of *Epfn* mutants and could potentially substitute for EPFN function.

It has been established that BMP signaling functions downstream from, or in parallel to, WNT signaling in the control of DV patterning (Soshnikova et al., 2003; Barrow et al., 2003). Remarkably, the DV phenotype of *Epfn* mutant limbs is reminiscent of the duplication of the digital tips seen upon *Noggin* overexpression in the AER (Wang et al., 2004) and is identical but milder to that exhibited by the conditional removal of *Bmpr1a* in the AER (Pajni-Underwood et al., 2007). Therefore, it is possible that EPFN mediates, at least partially, the connection between the WNT/b-CATENIN and the BMP signaling pathways in the limb ectoderm. The irregular expression of *Bmp4* in the mutant ectoderm strongly supports this hypothesis. It is also possible that EPFN interferes with BMP signaling in the ectoderm, independent of WNT. In this regard, the recent finding that follistatin, a BMP antagonist, is downregulated in cells overexpressing *Epfn* (Ruspita et al., 2008) is of particular interest.

AER maturation and distal limb defects

Our analysis shows that *Epfn* expression is required to achieve the elevated and compacted morphology typical of the mature AER. While it is well known that a mature morphology is not required for AER function (Errick and Saunders, 1974; 1976; Niswander et al., 1993; Fallon et al., 1994), the mechanisms that direct AER maturation are not completely understood (see for review Fernandez-Teran and Ros, 2007) and the specific way in which EPFN is required remains to be determined. The *Epfn* mutant AER phenotype, abnormally broad and flat and sometimes protruding into the mesoderm, is also described in a large number of mutants including those with loss-of-function of BMP in the limb ectoderm (Wang et al., 2004: Pajni-Underwood et al., 2007). Mutants with gain-of-function of WNT signaling in the ectoderm such as *doubleridge* (Adamska et al., 2003; MacDonald et al., 2004) and *Megf7/Lrp4* (Johnson et al., 2005) are characterized by a “double ridge” phenotype much more pronounced than *Epfn* mutants.

Interestingly, early deficiencies in the maturation of the AER normally result in very distal phenotypic defects generally confined to the digits or even digital tips (all the above mentioned mutants; Fernandez-Teran and Ros, 2007). One possible explanation for this observation is that the compact mature AER morphology, even if dispensable for signaling, is required for the paddle shape of the limb bud and subsequent achievement of the refined distal morphology of the limb as is discussed below (Dahmann and Basler, 1999).

Epiprofin and digit patterning

The *Epfn* mutant limb exhibits syndactyly in the forelimb and oligodactyly in the hindlimb, with digits 2–3 affected in the forelimb and digits 3–4 in the hindlimb. In *Epfn* mutant mice, the limb phenotype was always stronger in the hindlimb and the penetrance was higher on the left side, with many mutants showing the phenotype only on that side. The reason for this bias is presently unknown, but right or left-sided predominance of limb phenotypes is a relatively common observation (Dunn et al., 1997; Jiang et al., 1998; Katagiri et al., 1998; Adamska et al., 2003; Bell et al., 2003b; Johnson et al., 2005; Nam et al., 2007). This same phenotype has been recently reported in an independently generated knockout of *Sp6* (Hertveldt et al., 2008).

In the absence of EPFN, there is a tendency for the central digital rays to fuse, ranging from the simple mild cutaneous syndactyly to more severe synostosis and consequent oligodactyly. Synostosis is only observed in the mutant hindlimb, but it can show different degrees of severity, varying from osseous connection between two apposed, but still distinguishable, digits to a complete fusion of the two digits into a single thicker one. This observation supports the notion that syndactyly and oligodactyly may be different degrees of the same condition, particularly in this situation in which the synostotic digit is always thicker than normal.

The study of *Sox9* expression, which marks the chondrogenic condensations, clearly shows that the syndactyly in the *Epfn* hindlimbs is of early onset and is noticeably different from the late syndactyly that results from the failure of cell death to remove the interdigital mesenchyme (Lu et al., 2006). In the *Epfn* mutant, the hindlimb synostotic digits 3 and 4 arise together, from the base of the first phalanx, while the syndactyly of digits 2 and 3 in the forelimb is the result of the two digits being formed in close apposition. Therefore, since the syndactyly is established prior to the formation of the interdigital space, and before the normal onset of interdigital cell death, the cause of the phenotype cannot be reliant on a defect in interdigital cell death. However, in the forelimb, a reduction in the amount of interdigital cell death seems to play a role in the establishment of the cutaneous syndactyly.

Besides cell death, a reduced autopod cell mass has also been claimed as a causal factor of syndactyly (Talamillo et al., 2005). However, the fact that the synostotic digit is much thicker than a normal digit points to a patterning defect, rather than to a decrease in cell mass. At stages previous to the formation of the digital plate, *Epfn* mutant limb buds exhibit an altered shape, probably a consequence of the defect in AER maturation; changes in cell death and proliferation are not discernible. It is possible that the syndactyly in the *Epfn* mutant may result from a mechanical constraint caused by the wider non-linear AER, which results in a failure to establish a correct architecture of the digital plate and which then impedes the normal organization of the mesenchymal condensations and interdigital spaces. An alternative possibility is that the absence of *Epfn* from the limb ectoderm, in some way not presently determined, influences the mechanisms that control the pattern of digital condensations in the autopod. Indeed, we have observed altered gene expression, particularly that of *Bmp4*, *Msx2* and *Lmx1b*, which shows that the lack of *Epfn* in the limb ectoderm has an impact in the limb mesoderm. The observation that *Axin2* is downregulated in the dorsal and ventral mutant ectoderm indicates that EPFN may modulate WNT signaling by non-AER ectoderm, in addition to the AER.

Defects in digital pattern are among the most common birth malformations in humans. Interestingly, the limb phenotype in the absence of *Epfn* is comparable to the recently identified human mesoaxial synostotic syndactyly (MSSD, type IX syndactyly) (Malik et al., 2004; 2005) although the specific digits affected differs between human and mouse. This type of syndactyly is characterized by the mesoaxial reduction of fingers due to bony fusion of the third and fourth metacarpals bearing single phalanges. The similarity in the phenotype raises the question of whether they may represent the same condition. However, the gene responsible for the MSSD, although not yet identified, maps to human chromosome 17p13.3 (Malik et al. 2005), while human *Sp6* (the human orthologue of *Epfn*) maps to 17q21.32. Of the other eight types of genetic syndactyly classified in humans (Temtamy and McKusick, 1978; Goldstein et al. 1994), only Type I, or zygodactyly, has any similarities with the syndactyly in the *Epfn* mutant, although the digits affected are different. However, the locus and genes identified so far do not correspond to human *Sp6*. Therefore, it remains to be determined whether mutations in human *Sp6* are involved in some cases of human syndactyly.

Supplementary Material

Refer to Web version on PubMed Central for supplementary material.

Acknowledgments

We are very grateful to G. Martin and F. Mariani for the double *Fgf4*;*Fgf8* mutant embryos and to J. Galceran, A. Joyner, G. Martin, A. McMahon and C. Niehrs for generously providing reagents. This work was supported by grant BFU2008-00397 from the Spanish Ministry of Education and Science and grant API 05/27 from the IFIMAV to M.R., the Intramural Research Program of the NIDCR, NIH to Y.Y. and grant GIU05/27 from the University of the Basque Country to F.U. A.T. had a postdoctoral fellowship from the Instituto de Formación e Investigación Marqués de Valdecilla (IFIMAV). We acknowledge the excellent technical assistance of Marisa Junco.

REFERENCES

Adamska M, MacDonald BT, Meisler MH. Doubleridge, a mouse mutant with defective compaction of the apical ectodermal ridge and normal dorsal-ventral patterning of the limb. Dev. Biol. 2003; 255:350–362. [PubMed: 12648495]

Ahn K, Mishina Y, Hanks MC, Behringer RR, Crenshaw EB III. BMPR-IA signaling is required for the formation of the apical ectodermal ridge and dorsal-ventral patterning of the limb. Development. 2001; 128:4449–4461. [PubMed: 11714671]

Akiyama H, Chaboissier MC, Martin JF, Schedl A, de Crombrugghe B. The transcription factor Sox9 has essential roles in successive steps of the chondrocyte differentiation pathway and is required for expression of Sox5 and Sox6. Genes Dev. 2002; 16:2813–2828. [PubMed: 12414734]

Barrow JR, Thomas KR, Boussadia-Zahui O, Moore R, Kemler R, Cappecchi MR, McMahon AP. Ectodermal Wnt3/beta-catenin signaling is required for the establishment and maintenance of the apical ectodermal ridge. Genes Dev. 2003; 17:394–409. [PubMed: 12569130]

Bell SM, Schreiner CM, Waclaw RR, Campbell K, Potter SS, Scott WJ. Sp8 is crucial for limb outgrowth and neuropore closure. Proc. Natl. Acad. Sci. USA. 2003; 100:12195–12200. [PubMed: 14526104]

Bell SM, Schreiner CM, Hess KA, Anderson KP, Scott WJ. Asymmetric limb malformations in a new transgene insertional mutant, footless. Mechanisms of Development. 2003; 120:597–605. [PubMed: 12782276]

Bi W, Deng JM, Zhang Z, Behringer RR, de Crombrugghe B. Sox9 is required for cartilage formation. Nat. Genet. 1999; 22:85–89. [PubMed: 10319868]

Boulet AM, Moon AM, Arankiel BR, Capecchi MR. The roles of Fgf4 and Fgf8 in limb bud initiation and outgrowth. Dev. Biol. 2004; 273:361–372. [PubMed: 15328019]

Chen H, Johnson RL. Interactions between dorsal-ventral patterning genes lmx1b, engrailed-1 and wnt-7a in the vertebrate limb. Int. J. Dev. Biol. 2002; 46:937–941. [PubMed: 12455631]

Crossley PH, Martin GR. The mouse Fgf8 gene encodes a family of polipeptides and is expressed in regions that direct outgrowth and patterning in the developing embryo. Development. 1995; 121:439–451. [PubMed: 7768185]

Dahmann C, Basler K. Compartment boundaries: at the edge of development. Trends Genet. 1999; 15:320–326. [PubMed: 10431194]

Dudley AT, Ros MA, Tabin CJ. A re-examination of proximodistal patterning during vertebrate limb development. Nature. 2002; 418:539–544. [PubMed: 12152081]

Dunn NR, Winnier GE, Hargett LK, Schrick JJ, Fogo AB, Hogan BLM. Haploinsuffient phenotypes in Bmp4 heterozygous null mice and modification by mutations in Gli3 and Alx4. Dev. Biol. 1997; 188:235–247. [PubMed: 9268572]

Eblaghie MC, Lunn JS, Dickinson RJ, Munsterberg AE, Sanz-Ezquerro JJ, Farrell ER, Mathers J, Keyse SM, Storey K, Tickle C. Negative feedback regulation of FGF signaling levels by Pyst1/MKP3 in chick embryos. Curr. Biol. 2003; 13:1009–18. [PubMed: 12814546]

Errick JE, Saunders JW. Effects of an “inside-out” limb-bud ectoderm on development of the avian limb. Dev Biol. 1974; 41:338–351. [PubMed: 4452413]

Errick JE, Saunders JW. Limb outgrowth in the chick embryo induced by dissociated and reaggregated cells of the apical ectodermal ridge. Dev Biol. 1976; 50:26–34. [PubMed: 1269832]

Fallon JF, Lopez A, Ros MA, Olwin BB, Simandl BK. FGF-2: apical ectodermal ridge growth signal for chick limb development. Science. 1994; 264:104–107. [PubMed: 7908145]

Fernández-Terán MA, Ros MA. The Apical Ectodermal Ridge: morphological aspects and signaling pathways. Int. J. Dev. Biol. 2008; 52:857–71. [PubMed: 18956316]

Goldstein DJ, Kambouris M, Ward RE. Familial crossed polysyndactyly. Am. J. Med. Genet. 1994; 50:215–223. [PubMed: 8042663]

González-Sancho JM, Aguilera O, García JM, Pendás-Franco N, Peña C, Cal S, García de Herreros A, Bonilla F, Muñoz A. The Wnt antagonist DICKKOPF-1 gene is a downstream target of beta-catenin/TCF and is downregulated in human colon cancer. Oncogene. 2005; 24:1098–1103. [PubMed: 15592505]

Harrison SM, Houzelstein D, Dunwoodie SL, Beddington RSP. Sp5, a new member of the Sp1 family, is dynamically expressed during development and genetically interacts with Brachyury. Dev. Biol. 2000; 227:358–372. [PubMed: 11071760]

Hertveldt V, Louryan S, van Reeth T, Dreze P, van Vooren P, Szpirer J, Szpirer C. The development of several organs and appendages is impaired in mice lacking Sp6. Dev. Dyn. 2008; 237:883–92. [PubMed: 18297738]

Hill TP, Taketo. MM, Birchmeier W, Hartmann C. Multiple roles of mesenchymal beta-catenin during murine limb patterning. Development. 2006; 133:1219–1229. [PubMed: 16495310]

Jiang R, Lan Y, Chapman HD, Shawber C, Norton CR, Serreze DV, Weinmaster G, Gridley T. Defects in limb, craniofacial, and thymic development in Jagged2 mutant mice. Genes Dev. 1998; 12:1046–1057. [PubMed: 9531541]

Jho EH, Zhang T, Domon C, Joo CK, Freund JN, Costantini F. Wnt/beta-catenin/Tcf signaling induces the transcription of Axin2, a negative regulator of the signaling pathway. Mol Cell Biol. 2002; 22:1172–83. [PubMed: 11809808]

Johnson EB, Hammer RE, Herz J. Abnormal development of the apical ectodermal ridge and polysyndactyly in Megf7-deficient mice. Hum. Mol. Genet. 2005; 14:3523–3538. [PubMed: 16207730]

Kaczynski J, Cook T, Urrutia R. Sp1- and Krüppel-like transcription factors. Genome Biol. 2003; 4:206. [PubMed: 12620113]

Kadonaga JT, Carner KR, Masiarz FR, Tjian R. Isolation of cDNA encoding transcription factor Sp1 and functional analysis of the DNA binding domain. Cell. 1987; 51:1079–1090. [PubMed: 3319186]

Katagiri T, Boorla S, Frendo JL, Hogan B, Karsenty G. Skeletal abnormalities in double heterozygous Bmp4 and Bmp7 mice. Dev. Genetics. 1998; 22:340–348.

Kawakami Y, Capdevila J, Buscher D, Itoh T, Rodriguez Esteban C, Izpisua-Belmonte JC. WNT signals control FGF-dependent limb initiation and AER induction in the chick embryo. Cell. 2001; 104:891–900. [PubMed: 11290326]

Kawakami Y, Rodriguez-Leon J, Koth CM, Buscher D, Itoh T, Raya A, Ng JK, Esteban CR, Takahashi S, Henrique D, et al. MKP3 mediates the cellular response to FGF8 signalling in the vertebrate limb. Nat. Cell. Biol. 2003; 5:513–9. [PubMed: 12766772]

Kawakami Y, Esteban CR, Matsui T, Rodriguez-Leon J, Kato S, Izpisua-Belmonte JC. Sp8 and Sp9, two closely buttonhead-like transcription factors, regulate Fgf8 expression and limb outgrowth in vertebrate embryos. Development. 2004; 131:4763–4774. [PubMed: 15358670]

Kimmel R, Turnbull DH, Blanquet V, Wolfgang W, Loomis CA, Joyner AL. Two lineage boundaries coordinate vertebrate apical ectodermal ridge formation. Genes Dev. 2000; 14:1377–1389. [PubMed: 10837030]

Loomis CA, Kimmel RA, Tong CX, Michaud J, Joyner AL. Analysis of the genetic pathway leading to formation of ectopic apical ectodermal ridges in mouse Engrailed-1 mutant limbs. Development. 1998; 125:1137–1148. [PubMed: 9463360]

Lu P, Minowada G, Martin GR. Increasing Fgf4 expression in the mouse limb bud causes polysyndactyly and rescues the skeletal defect that result from loss of Fgf8 function. Development. 2006; 133:33–42. [PubMed: 16308330]

Lustig B, Jerchow B, Sachs M, Weiler S, Pietsch T, Karsten U, van de Wetering M, Clevers H, Schlag PM, Birchmeier W, Behrens J. Negative feedback loop of Wnt signaling through upregulation of conductin/axin2 in colorectal and liver tumors. Mol Cell Biol. 2002; 22:1184–93. [PubMed: 11809809]

MacDonald BT, Adamska M, Meisle MH. Hypomorphic expression of Dkk1in the doubleridgemouse: dose dependence and compensatory interactions withLrp6. Development. 2004; 131:2543–2552. [PubMed: 15115753]

Malik S, Arshad M, Amin-Ud-Din M, Oeffner F, Dempfle A, Haque S, Koch MC, Ahmad W, Grzeschik KH. A novel type of autosomal recessive syndactyly: clinical and molecular studies in a family of Pakistani origin. Am. J. Med. Genet. A. 2004; 126:61–67. [PubMed: 15039974]

Malik S, Percin FE, Ahmad W, Percin S, Akarsu NA, Koch MC, Grezeschik KH. Autosomal recessive mesoaxial synostotic syndactyly with phalangeal reduction maps to chromosome 17p13.3. Am. J. Med. Genet. A. 2005; 134:404–408. [PubMed: 15779011]

Mariani FV, Ahn CP, Martin GR. Genetic evidence that FGFs have an instructive role in limb proximo-distal patterning. Nature. 2008; 453:401–405. [PubMed: 18449196]

Martin GR. The roles of FGFs in the early development of vertebrate limbs. Genes Dev. 1998; 12:1571–1586. [PubMed: 9620845]

Nakamura T, Unda F, de-Vega S, Vilaxa A, Fukumoto S, Yamada KM, Yamada Y. The Krüppel-like factor epiprofin is expressed by epithelium of developing theeth, hair follicles, and limb buds and promotes cell proliferation. J. Biol.Chem. 2004; 279:626–634. [PubMed: 14551215]

Nakamura T, de Vega S, Fukumoto S, Jimenez L, Unda F, Yamada Y. Transcription factor epiprofin is essential for tooth morphogenesis by regulating epithelial cell fate and tooth number. J. Biol. Chem. 2008; 283:4825–4833. [PubMed: 18156176]

Nam JS, Park E, Turcotte TJ, Palencia S, Zhan X, Lee J, Yun K, Funk WD, Yoon JK. Mouse R-spondin2 is required for apical ectodermal ridge maintenance in the hindlimb. Dev. Biol. 2007; 311:124–135. [PubMed: 17904116]

Niida A, Hiroko T, Kasai M, Furukawa Y, Nakamura Y, Suzuki Y, Sugano S, Akiyama T. Dkk1, a negative regulator of Wnt signaling, is a target of the b-catenin/TCF pathway. Oncogene. 2004; 23:8520–8526. [PubMed: 15378020]

Niswander L, Tickle C, Vogel A, Booth I, Martin GR. FGF-4 replaces the apical ectodermal ridge and direct outgrowth and patterning of the limb. Cell. 1993; 75:579–587. [PubMed: 8221896]

Niswander L. Pattern formation: old models out on a limb. Nat. Rev. Genet. 2003; 4:133–143. [PubMed: 12560810]

Ovchinnikov DA, Selever J, Wang Y, Chen YT, Mishina Y, Martin JF, Behringer RR. BMP receptor type IA in limb bud mesenchyme regulates diatal outgrowth and patterning. Dev. Biol. 2006; 295:103–115. [PubMed: 16630606]

Pajni-Underwood S, Wilson CP, Elder C, Michina Y, Lewandoski M. BMP signals control limb bud interdigital programmed cell death by regulating FGF signaling. Development. 2007; 134:2359–2368. [PubMed: 17537800]

Parr BA, McMahon AP. Dorsalizing signal Wnt-7a required for normal polarity of D-V and A-P axes of mouse limb. Nature. 1995; 374:350–3. [PubMed: 7885472]

Pizette S, Abate-Shen C, Niswander L. BMP controls proximodistal outgrowth, via induction of the apical ectodermal ridge, and dorsoventral patterning in the vertebrate limb. Development. 2001; 128:4463–4474. [PubMed: 11714672]

Rowe DA, Cairns JM, Fallon JF. Spatial and temporal patterns of cell death in limb bud mesoderm after apical ectodermal ridge removal. Dev. Biol. 1982; 93:83–91. [PubMed: 7128939]

Ruspita I, Moyoshi K, Muto T, Abe K, Horiguchi T, Noma T. Sp6 downregulation of follistatin gene expression in ameloblasts. The Journal of Medical Investigation. 2008; 55:87–98. [PubMed: 18319550]

Saunders JW Jr. The proximo-distal sequence of origin of the parts of the chick wing and the role of the ectoderm. J. Exp. Zool. 1948; 108:363–403. [PubMed: 18882505]

Sekine K, Ohuchi H, Fujiwara M, Yamasaki M, Yoshizawa T, Sato T, Yagishita N, Matsui D, Koga Y, Ithoh N, Kato S. Fgf10 is essential for limb and lung formation. Nat. Genetic. 1999; 21:138–141.

Selever J, Liu W, Lu M, Behringer RR, Martin JF. Bmp4 in limb bud mesoderm regulates digit pattern by controlling AER development. Dev. Biol. 2004; 276:268–279. [PubMed: 15581864]

Soshnikova N, Zechner D, Huelsken J, Mishina Y, Behringer RR, Taketo MM, Crenshaw EB 3rd. Birchmeier W. Genetic interaction between Wnt/b-catenin and BMP receptor signaling during formation of the AER and the dorsal-ventral axis in the limb. Genes Dev. 2003; 17:1963–1968. [PubMed: 12923052]

Sun X, Mariani FV, Martin GR. Functions of FGF signalling from the apical ectodermal ridge in limb development. Nature. 2002; 418:501–508. [PubMed: 12152071]

Suske G, Bruford E, Philipsen S. Mammalian SP/KLF transcription factors: Bring in the family. Genomics. 2005; 85:551–556. [PubMed: 15820306]

Talamillo A, Bastida MF, Fernandez-Teran M, Ros MA. The developing limb and the control of the number of digits. Clin. Genet. 2005; 67:143–153. [PubMed: 15679824]

Temtamy SA, McKusick VA. The genetics of hand malformations. Birth Defects Orig. Artic. Ser. 1978; 14:1–619.

Tickle C. Patterning systems-From one end of the limb to the other. Developmental Cell. 2003; 4:449–458. [PubMed: 12689585]

Treichel D, Becker M, Gruss P. The novel transcription factor gene Sp5 exhibits a dynamic and highly restricted expression pattern during mouse embryogenesis. Mech. Dev. 2001; 101:175–179. [PubMed: 11231070]

Treichel D, Schock F, Jackle H, Gruss P, Mansouri A. mBtd is required to maintain signalling during murine limb development. Genes Dev. 2003; 17:2630–2635. [PubMed: 14597661]

Wang CK, Omi M, Ferrari D, Cheng HC, Lizarraga G, Chin HJ, Upholt WB, Dealy CN, Kosher RA. Function of BMPs in the apical ectoderm of the developing mouse limb. Dev. Biol. 2004; 269:109–122. [PubMed: 15081361]

Witte F, Dokas J, Neuendorf F, Mundlos S, Stricker S. Comprehensive expression analysis of all Wnt genes and their major secreted antagonists during mouse limb development and cartilage differentiation. Gene Expression Patterns. 2008; 9(2009):215–223. [PubMed: 19185060]

Wimmer EA, Jackle H, Pfeifle C, Cohen SM. A Drosophila homologue of human Sp1 is a head-specific segmentation gene. Nature. 1993; 366:690–694. [PubMed: 8259212]

Zuñiga A, Haramis AP, McMahon AP, Zeller R. Signal relay by BMP antagonism controls the SHH/FGF4 feedback loop in vertebrate limb buds. Nature. 1999; 401:598–602. [PubMed: 10524628]

Zuzarte-Luis V, Hurle JM. Programmed cell death in the embryonic vertebrate limb. Sem. Cell Dev. Biol. 2005; 16:261–269.

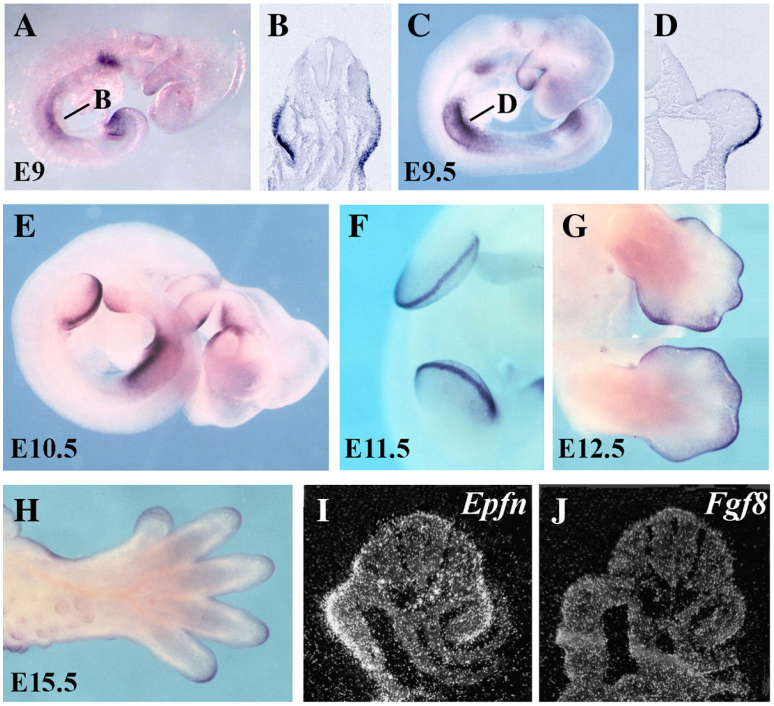

Figure 1. Expression pattern of *Epiprofin* during mouse limb bud development

Whole-mount *in situ* hybridization was performed on wild-type embryos of the indicated age with an *Epfn* antisense riboprobe. (A–D) At E9 and E9.5 *Epfn* is expressed in the presumptive fore- and hindlimb ectoderm as shown in the whole mounts and corresponding sections at the forelimb level as marked in the corresponding whole mount (B, D). At E10.5 (E) and E11.5 (F) *Epfn* expression is predominantly confined to the AER. At E12.5 (G) *Epfn* expression continues in the AER and extends into the dorsal and ventral ectoderm particularly at digital tips. At 14.5 (H) *Epfn* expression still occurs in the ectoderm of the digital tips. (I, J) show two consecutive serial sections (6 mm apart) through the presumptive forelimb of an E9 mouse embryo, showing *Epfn* expression in the limb field ectoderm (I), while *Fgf8* expression has not yet been activated (J) at this stage.

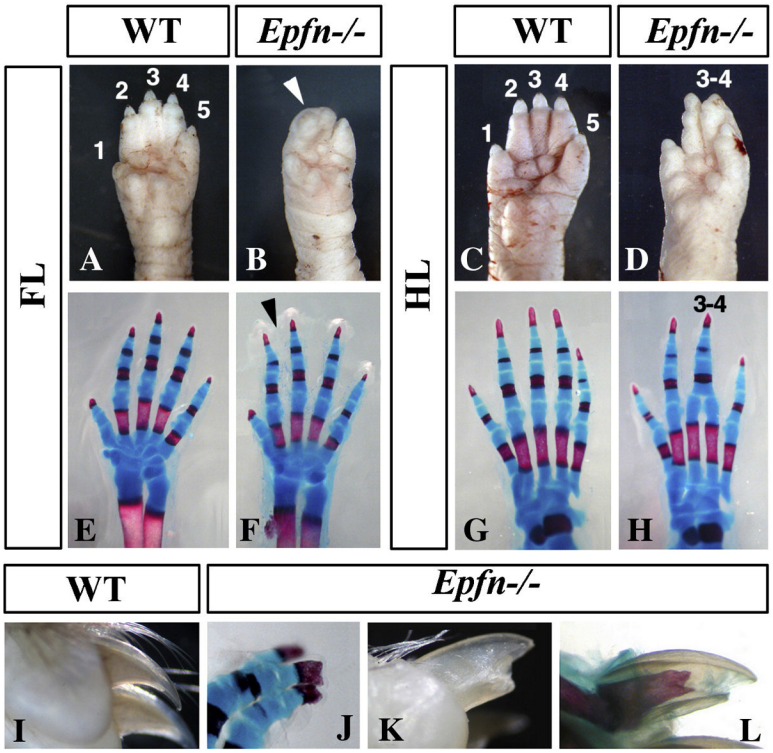

Figure 2. Limb phenotype of *Epiprofin* mutant embryos

(A–H) External morphology (A–C) and skeletal pattern (E–H) of newborn control and mutant fore- and hindlimbs, as indicated. Note the soft tissue syndactyly in the forelimb (arrowhead in B) and the oligodactyly of four digits in the hindlimb (D and H). (I–L) Morphology of the digital tip of 6-week-old control (I) and mutant (K–L) limbs. (J) is a skeletal preparation of the broader distal tip of the ungeal phalanx in a newborn. The numbers in some panels indicate the identity of the digits.

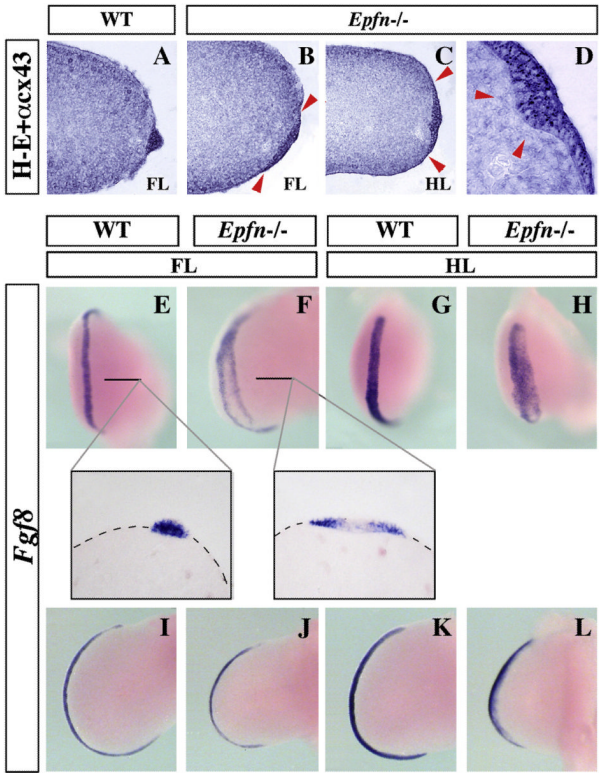

Figure 3. Abnormal AER morphology and *Fgf8* expression in the *Epfn* mutant limb

(A–D) Histological sections showing the AER morphology in a E11.5 wild type forelimb (A) and mutant fore- (B) and hindlimb (C–D). The mutant AER, delimited by arrowheads in (B) and (C), is expanded in the DV axis, lacks the typical elevation and sometimes protrudes into the mesenchyme (arrowheads in D). (E–L) are whole mount *in situ* hybridizations showing the expression pattern of *Fgf8* in control and mutant limbs, as indicated at the top of each panel. The inserts show longitudinal sections at the level indicated in E and F.

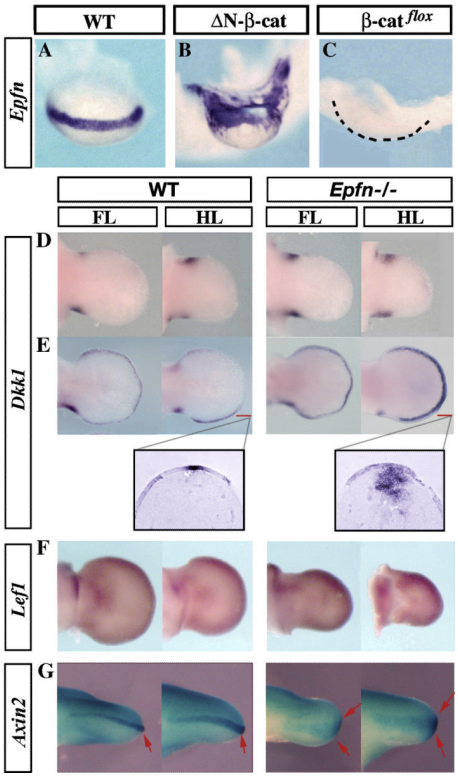

Figure 4. *Epiprofin* and WNT/b-CATENIN signaling

(A–C) Whole mount *in situ* hybridization showing the expression pattern of *Epfn* in the hindlimb of wild type (A), gain-of-function mutant of *b-catenin* (*Brn4Cre;DN-b-catenin*) (B), and loss-of-function mutant of *b-catenin* (*Brn4Cre;b -catenin* $^{flox/flox}$). The dashed line in (C) marks the contour of the mutant hindlimb that does not express *Epfn*. (D–E) *Dkk1* pattern of expression is shown at E11 (top row) and E12 (bottom row) in WT and mutant limbs. *Dkk1* expression is increased in the mutant distal hindlimb mesoderm as can be clearly appreciated in the longitudinal sections shown in the corresponding inserts. (F) The pattern of *Lef1* expression is similar in normal and mutant limbs. (G) *Axin2* expression was analyzed in compound mice expressing *lacZ* under the control of the *Axin2* promoter. *Axin2* expression is reduced in the mutant ectoderm and AER (arrows) compared with the control. Anterior views of the limbs are presented.

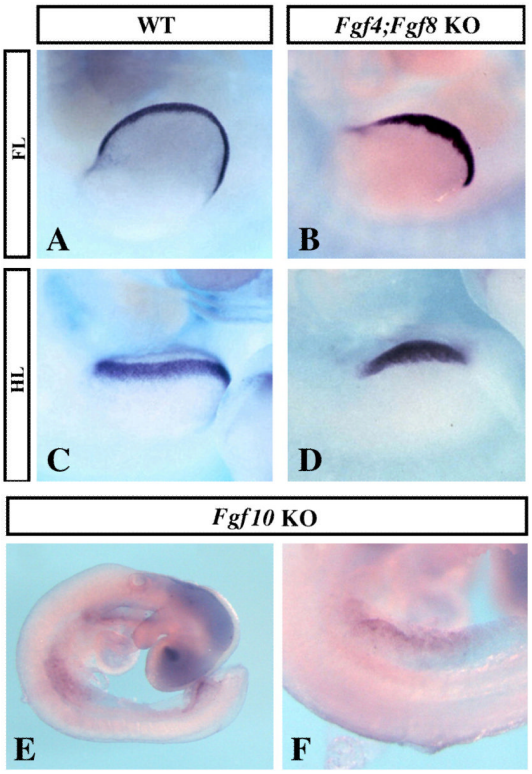

Figure 5. Epiprofin expression in the limb ectoderm is independent of FGF signaling

(A–D) Whole mount *in situ* hybridization for *Epfn* in E10 wild type and *Msx2Cre;Fgf4;Fgf8* double mutants, as indicated. (E–F) Whole mount *in situ* hybridization for *Epfn* in an E9 *Fgf10* mutant, showing normal expression in the limb ectoderm. (F) is a magnification of (E).

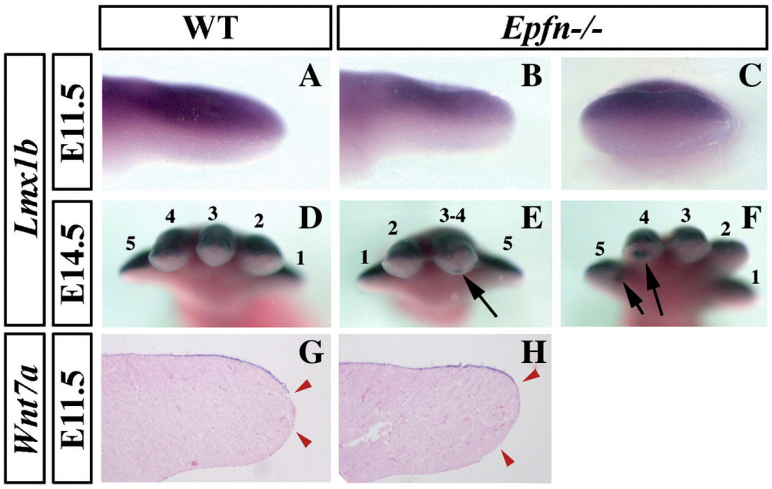

Figure 6. Dorsoventral patterning defects in *Epiprofin* mutant limbs

At E11.5, the expression domain of *Lmx1b* in the mutant hindlimb is properly restricted to the dorsal mesoderm (B–C), as in control limbs (A). At later stages (E14.5), occasional patches of ectopic *Lmx1b* expression, indicated by arrows, are detected in mutant (E–F), but not in wild type limbs (D). At E11.5, wild type and mutant limbs show similar expression pattern of *Wnt7a* in the dorsal ectoderm (G–H). (A) and (B) are lateral views, (C–F) show views from the tip of the limb, and (G–H) are longitudinal sections. The numbers in some panels indicate the identity of the digits.

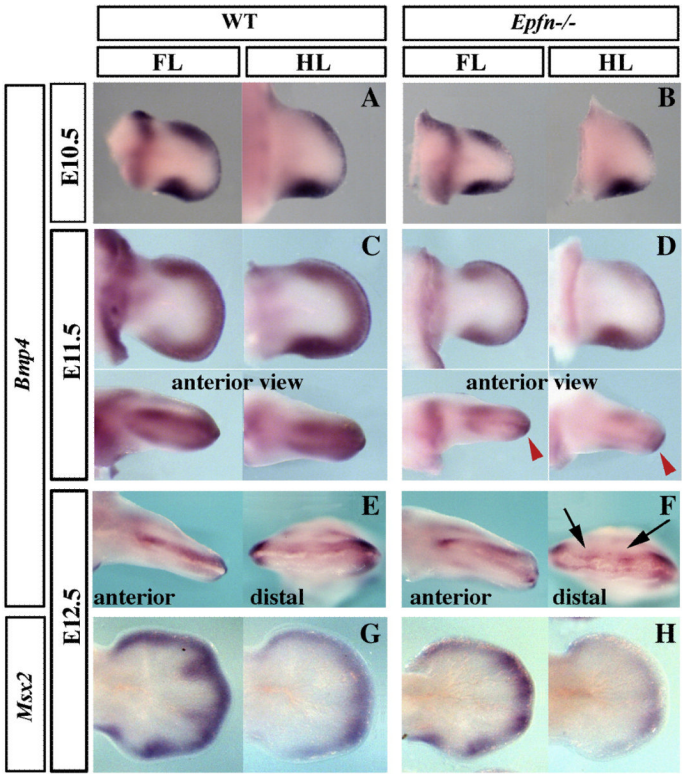

Figure 7. *Bmp4* expression and signaling in *Epiprofin* mutants

At E10.5, the expression of *Bmp4* in the mutant fore and hindlimb is slightly downregulated (B) compared to wild type (A). At E11.5, this downregulation is clearer (C–D) shown in ventral views at the top and in anterior views at the bottom of the panel, as indicated. At E12.5, *Bmp4* expression in the ectoderm appears patchy particularly in the hindlimbs shown in anterior and distal views (E, F). At E12.5, *Msx2* expression is also downregulated in mutant limbs, confirming the reduction in BMP signaling at E12.5 (G–H).